*Article*

# Development of a Unique Technology for the Pyrolysis of Rice Husk Biochar for Promising Heavy Metal Remediation

Ilia Lobzenko [1], Marina Burachevskaya [1], Inna Zamulina [1], Anatoly Barakhov [1], Tatiana Bauer [1], Saglara Mandzhieva [1], Svetlana Sushkova [1], Tatiana Minkina [1], Andrey Tereschenko [1], Valery Kalinichenko [2], Oleg Khroniuk [1] and Vishnu D. Rajput [1,*]

[1] Academy of Biology and Biotechnology named after D.I. Ivanovsky, Southern Federal University, 344006 Rostov-on-Don, Russia
[2] Institute of Fertility of Soils of South Russia, 346493 Persianovka, Russia
[*] Correspondence: rajput.vishnu@gmail.com; Tel.: +7-918-589-00-93

**Abstract:** Due to anthropogenic activities, potentially toxic elements cause severe soil pollution worldwide. Therefore, remediation of contaminated soils is exigent and imperative. One cost-effective and environmentally friendly remediation approach is the application of biochar, which is a solid carbonaceous material. Biochar degrades slowly in soil and can persist there for thousands of years, according to various estimations. In addition, coal obtained from crop wastes has a developed porous structure, a high specific surface area, and does not contain toxic compounds such as heavy metals and polycyclic aromatic hydrocarbons. Biochar with optimal values for specific surface area and porosity was obtained from rice husk by stepwise pyrolysis. The pyrolysis parameters such as the heating rate (11 °C·min⁻¹), temperature (700 °C), and holding time (45 min) were established. At the same time, the surface area of the biochar increased by almost three times with a change in the pyrolysis conditions. As a part of this research, the efficacy of adsorption of Cu(II) from Haplic Chernozem using biochar made from rice husk was examined. The Langmuir and Freundlich models were employed to describe the adsorption data. The isotherm data of heavy metals was better fitted to the Langmuir adsorption model. The addition of rice husk biochar to the soil presented greater removal efficiencies of Cu(II) than soil in pure form. The analysis of the structural characteristics of the sorbent suggest that this material may work efficiently for the restoration of contaminated soil.

**Keywords:** rice husk; stepwise pyrolysis; sorption characteristics; degree of aromaticity; biochar

## 1. Introduction

Recently, the world community has been paying more attention to the problems of conservation and rational use of soils [1]. This is evident in the inclusion of soil conservation and sustainable land use in the United Nations (UN) sustainable development plan [2]. Rapid global industrial development, intensive agricultural practices, and land-use change have resulted in soil degradation and a significantly increased risk of soil contamination by heavy metals (HMs) [3–5]. Fast industrialization and disorganized urbanization, together with long-term use of large amounts of fertilizers and pesticides, has resulted in accumulation of HMs in soil [6]. The main feature of HMs as pollutants is that they are poorly biodegradable, which leads to their accumulation in soils and an increase in their toxic effects over time [7]. Numerous studies have shown that an increase in the content of HMs in the soil increases their bioavailability for plants, and consequently, the potential danger to the environment and human health [2,8,9].

One of the promising methods for combating soil pollution with HMs is to decrease their toxic effect by reducing their bioavailability [1]. To achieve this goal, it is proposed to use more environmentally friendly and cost-effective remediation methods, such as

remediation by sorption. Several studies have suggested employing carbon sorbents such as biochar for these applications [10–12]. Biochar degrades slowly in soil and can persist there for thousands of years, according to various estimations [13]. In addition, coal obtained from crop wastes has a developed porous structure, a high specific surface area, and does not contain toxic compounds such as HMs and polycyclic aromatic hydrocarbons (PAHs) [12]. Due to its porous structure and surface functional groups, biochar has become a promising solution to various environmental problems [14]. In addition to being a soil cleaner, biochar can also serve as a fertilizer for agricultural plants by increasing the biological activity of soils, helping to retain moisture available to plants, and improving the chemical and physical characteristics of soil [12,15].

The main approach for obtaining biochar is the pyrolysis of plant residues from agricultural waste, therefore biochar production is one of the ways to cost-effectively process these wastes [16]. The use of regional agricultural waste is often observed [17]. The superiority of this type of material lies in the fact that it is inexpensive or even free, and is available in abundance, especially in countries with strong agricultural economies such as Russia. Rice is a staple food in most regions of Asia, which is home to more than 90% of the world's rice production and consumption [18]. As another agricultural country in the world, Russia produces more than 1 million tons of rice husk every year. However, rice husks are low in volume density, difficult to transport and store, hard textured, slow to decompose in soil, and of low nutritional value [19]. Simple incineration is obviously not conducive to environmental and ecological protection, and reasonable and value-added utilization of such large amounts of rice husk has become an urgent issue. In addition, rice husk contains a large amount of inert silicon, making it an excellent precursor for preparing biochar [20]. Biochar generated from rice husk has been reported to exhibit multiple functions and be a low-cost material [21].

The properties of biochar largely depend on the type of feedstocks and on pyrolysis conditions such as temperature, heating rate, and duration [22,23]. With a change in the final temperature of pyrolysis, and the time of exposure at the final temperature, there are changes in the carbon supply of the biochar, its potential stability in the soil, and its sorption characteristics [24].

The goal of this study was to develop a method for obtaining biochar with desired characteristics from rice husk. The production of this material will help solve several problems by eliminating the accumulation of regional crop waste and creating a unique material that is useful both in soil restoration and in agriculture.

## 2. Materials and Methods

As a source of rice husk, waste from the production of rice (*Oryza sativa* L.) was collected from Proletarsky district, Rostov region, Russia. The rice was represented by the Boyarin variety, which still occupies the main acreage in the Rostov region. Rice husk was carefully washed three times with tap water and once with distilled water to remove impurities. After that, the husk was dried at 105 °C in the oven for 3 h until it was completely dry. An aliquot of the feedstock (100 g) was loaded into a sealed 2 L stainless steel vessel which was itself placed inside a muffle furnace under limited oxygen conditions. Biochar was produced using a stepwise pyrolysis method (Figure 1). The uniqueness of this method lies in the selection of specific pyrolysis conditions for a certain raw material (in this study, rice husk) in order to obtain biochar with optimal structural characteristics. However, in general, the pyrolysis conditions are different for each type of raw material. To establish the optimal conditions for this process, an experiment was set up with different values for heating rate, final temperature, and holding time capacity. The heating rate varied from 8 to 11 °°C·min$^{-1}$, the final temperatures were 500 °C and 700 °C, and the holding time at the final pyrolysis temperature varied from 15 to 45 min. The mass yield of the final product and the specific surface area were key indicators for determining the most optimal pyrolysis conditions. The experiment was divided into 3 stages. At the first

stage, only the effect of holding time at the final temperature was considered. At the second stage, the influence of the heating rate was considered. At the third stage, the influence of the final pyrolysis temperature was considered. The experiment was replicated three times at each stage. At the end of the carbonization, the biochar's weight and feedstock mass loss (%) were calculated. The recorded weight losses for the obtained samples were found to be about 52.5–62.9%, depending on the pyrolysis conditions. In total, 10 kg of rice husks were processed to obtain biochar samples.
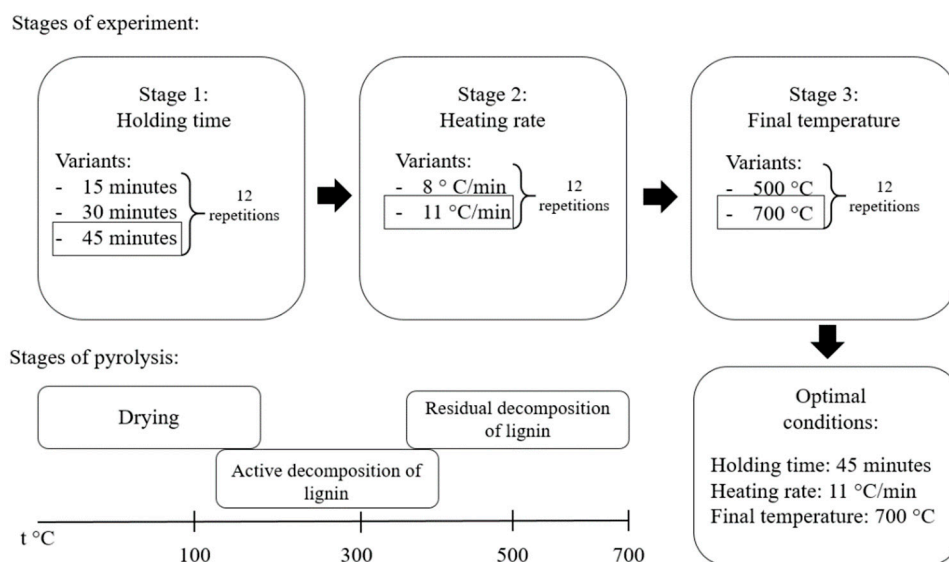


**Figure 1.** Scheme of experiment.

The morphology of the biochar obtained under the most optimal conditions was studied using scanning electron microscopy (SEM) and compared with the morphology of the raw material. The images were taken with a Carl Zeiss EVO-40 XVP scanning electron microscope. The imaging was carried out under standard conditions for non-conductive and low-contrast samples (low vacuum, 15 kV, increased emission), and the conductive layer was not deposited (the study of morphology under inactive conditions).

The contents of C, H, and N (in %) of the resulting sorbent were determined by high-temperature catalytic combustion on a TOC-L CPN Shimadzu (Japan) analyzer to establish the ratio of the main elements. The oxygen content was calculated by difference:

$$O\ (\%) = 100 - (ash\ content + C + H + N) \tag{1}$$

After determining the O content, the atomic ratios of the main elements were calculated. Subsequently, the biochar samples were heated for 6 h at 800 °C to determine ash content, according to the following formula [25]:

$$Ash\ (\%)\ =\ \frac{weight\ of\ ashed\ sample}{dry\ weight\ of\ sample} \times 100 \tag{2}$$

The high-temperature catalytic oxidation technique complies with the following standardizations: EN 1484, ISO 20236, ISO 8245, EN 12,260 (using TNM-L option), and EN 15,936 (using SSM-5000A option). Grade A coal (GOST 7657-84) was used as a reference material with a carbon content of at least 90% and an established elemental composition. Duplicates and reagent blanks were also used as a part of the quality control. The accuracy of the obtained results was repeatedly confirmed by international intercalibrations.

In addition, an analysis of the sorption characteristics was carried out with an ASAP 2020 Micrometrics volumetric analyzer. The surface and porosity parameters were calculated using the Brunauer–Emmett–Teller (BET) method for N2 in the range of equilibrium

values P/P0 = 0.05-0.33. The volumes of micro- ($V_{micro}$), meso- ($V_{meso}$), and macropores ($V_{macro}$) as well as the total limiting volume of the adsorption space ($V\Sigma$) were calculated. The study of these parameters is important for evaluating the possibility of using the resulting biochar as a means of remediation in contaminated soils. We conducted model experiments to study the sorption capacity of biochar for HMs (on the example of Cu). For this purpose, an experimental sample of Haplic Chernozem (Clayic) (Rostov region, Russia) was taken from the surface of virgin soil (0–20 cm). This soil was characterized by the following physicochemical properties: Corg 3.7%; $CaCO_3$ 0.1%; $pH_{H2O}$ 7.3; cation exchange capacity (CEC) 37.1 cmol(+) kg$^{-1}$; exchangeable cations (cmol(+) kg$^{-1}$): $Ca^{2+}$ 31.0, $Mg^{2+}$ 4.5; clay particles (<0.01 mm) 53.1%; clay particles (<0.001 mm) 32.4%.

Samples of biochar from rice husk at a dose of 2.5% of the soil mass were added separately to the soil samples. In the pre-sorption experiments with biochar in an equilibrium solution, the concentration of metals was below the detection limit, which indicates a high absorption capacity of the biochar. The specific adsorption of Cu by soil in pure form and soil with biochar was performed by adding 5.0 g constant weight of the sorbents and flexible concentrations of metal in the form of $Cu(NO_3)_2 \times 3H_2O$ within the range of 0.05 to 1.0 mM l$^{-1}$. The liquid–solid phase mass ratio was 1:10. Following 1 h of shaking, the suspensions were filtered using a blue-ribbon filter and allowed to settle for 1 day to reach equilibrium. Atomic absorption spectrometry (AAS) atomization was used to estimate the equilibrium concentrations of metal ions in an aqueous solution (with electrothermal and polarizing Zeeman correction of non-selective absorption (MGA-915MD, Lyumeks, St. Petersburg, Russia)). The difference between the additional quantity and the concentration recorded in the equilibrium solution was used to calculate the amount of metal adsorbed by the solid phase:

$$C_{ad} = \frac{(C_i - C_{eq}) \cdot V}{m} \tag{3}$$

where $C_{ad}$ is the amount of metal adsorbed by a unit sorbent mass (mM·kg$^{-1}$); $C_i$ is the initial metal concentration in solution (mM); $C_{eq}$ is the metal concentration in solution at equilibrium (mM); V is volume of the solution (cm$^3$); and m is the mass of the sorbent (g). The information gathered was used to create the $C_{eq}$–$C_{ad}$ plot.

Two important adsorption isotherms, namely Langmuir and Freundlich, were tested for fitting the experimental data. The Langmuir model assumes monolayer adsorption of ions onto homogeneous adsorption sites [26]. It also enables the calculation of the maximum adsorption capacities of the adsorbents to optimize their use. This model of an isotherm is as shown in Equation (4):

$$C_{ad} = \frac{C_m K_L}{1 + K_L C_e} \tag{4}$$

where $C_m$ is the maximum adsorption capacity for the metal (mM·kg$^{-1}$); $C_e$ is the concentration of metal at equilibrium (mM·L$^{-1}$); and $K_L$ is the constant of the Langmuir model (L·mM$^{-1}$).

The Freundlich model assumes multilayer adsorption on heterogeneous adsorption sites [26]. This model of an isotherm is given by the following equation:

$$C_{ad} = K_F C_e^n \tag{5}$$

where $K_F$ and n are the Freundlich adsorption capacity (L·kg$^{-1}$) and the Freundlich constant related to the surface heterogeneity, respectively. The $K_F$ coefficient in the Freundlich model is a measure of the relative absorption capacity, and the dimensionless parameter n makes it possible to reveal the energy inhomogeneity of the reaction centers on the sorbing surface. It can vary in the range $0 < n \le 1$. When the value of n approaches 0, the inhomogeneity of the sorption centers increases. When n approaches 1, it decreases.

All laboratory experiments were performed in triplicates. The statistical analysis was performed using SigmaPlot 12.5 and STATISTICA software packages with a confidence

coefficient of 0.95. Origin (OriginLab, USA) was used to assist simulations of the Langmuir and Freundlich models. The correlation coefficient ($R^2$) was used to assess the model's accuracy.

## 3. Results

The yield of biochar from rice husk was found to be about 37.1–47.5%, and ash content was 12.7–28.3%, depending on the pyrolysis conditions (Table 1). The first stage of the experiment established the optimal holding time of the raw material at the final pyrolysis temperature. Pyrolysis occurred at a heating rate of 8 °C·min⁻¹, and the final temperature was 500 °C. These values were chosen as the minimum of the above. When the holding time was changed from 15 to 45 min, there was a tendency towards a slight decrease in the yield of biochar from rice husk (47.5 to 43.1%) with a significant increase in the surface area: from 135 to 186 m²·g⁻¹ (Table 1).

**Table 1.** Characteristics of biochar at different stages of experiment.

| Stage | Final Temperature, °C | Heating Rate, °C·min⁻¹ | Holding Time, min | Product Yield, % | Ash Content, % | $S_{BET}$, m²·g⁻¹ |
|---|---|---|---|---|---|---|
| Stage 1 | 500 | 8 | 15 | 47.5 | 28.3 | 135 ± 9 * |
| | 500 | 8 | 30 | 45.2 | 26.2 | 164 ± 11 |
| | 500 | 8 | 45 | 43.1 | 18.0 | 186 ± 13 |
| Stage 2 | 500 | 8 | 45 | 43.1 | 17.6 | 184 ± 10 |
| | 500 | 11 | 45 | 42.3 | 14.0 | 278 ± 17 |
| Stage 3 | 500 | 11 | 45 | 42.3 | 14.3 | 279 ± 19 |
| | 700 | 11 | 45 | 37.1 | 12.7 | 398 ± 21 |

* Values represented are averages ± standard deviation; the number of replicates corresponded to three (*n* = 3).

The second stage established the optimal heating rate of the raw material. At this stage, pyrolysis occurred at a final temperature of 500 °C and holding time of 45 min (Table 1). The results showed that the heating rate increased, and the surface area of the product increased from 186 to 278 m²·g⁻¹. The product yield did not change significantly (43.1% at 8 °C·min⁻¹and 42.3% at 11 °C·min⁻¹).

During the third stage of the experiment, the optimal final pyrolysis temperature was established. An increase in the final pyrolysis temperature from 500 to 700 °C led to an increase in the surface area. Thus, at a heating rate of 11 °C·min⁻¹, the specific surface area was 398 m²·g⁻¹. At the same time, the product yield decreased 37.1% due to the increase in temperature. For biochar obtained with this technology, an analysis of the sorption volume of pores of various sizes was carried out (Table 2). The mesopores of this biochar have the largest volume—1.59 cm³·g⁻¹. The volumes of macro- and microspores differed insignificantly and amounted to 0.68 cm³·g⁻¹and 0.61 cm³·g⁻¹, respectively. The total pore volume of the resulting biochar was 2.88 cm³·g⁻¹.

**Table 2.** Sorption characteristics and elemental composition of biochar obtained under optimal pyrolysis conditions.

| Sorption Characteristics | | | | |
|---|---|---|---|---|
| | | Pore volume (cm$^3 \cdot$g$^{-1}$) | | |
| $S_{BET}$ (m$^2 \cdot$g$^{-1}$) | $\Sigma$V | V$_{macro}$ >50 nm | V$_{meso}$ 2–50 nm | V$_{micro}$ <2 nm |
| 398 ± 21 * | 2.88 | 0.61 ± 0.05 | 1.59 ± 0.11 | 0.68 ± 0.04 |

| Elemental analysis | | | | | | | | |
|---|---|---|---|---|---|---|---|---|
| Content of elements and ash, % | | | | | | Atomic Relations | | |
| C | H | N | O | Ash | H/C | O/C | (N+O)/C | C/N |
| 70.4 | 2.1 | 3.0 | 11.8 | 12.7 | 0.36 | 0.13 | 0.15 | 34.10 |

* Values represented are averages ± standard deviation; the number of replicates corresponded to three ($n$ = 3).

As can be seen from the microphotographs, the surface of the rice husk had small irregularities that formed a network of peculiar tubules (Figure 2). Numerous but shallow folds were also present, and the pores were not visible in the photographs. The surface of the biochar made from rice husk had pronounced alternating irregularities that formed a network of cells. In addition, the photographs show numerous deep folds that can act as sorption centers.



**(A)**          **(B)**
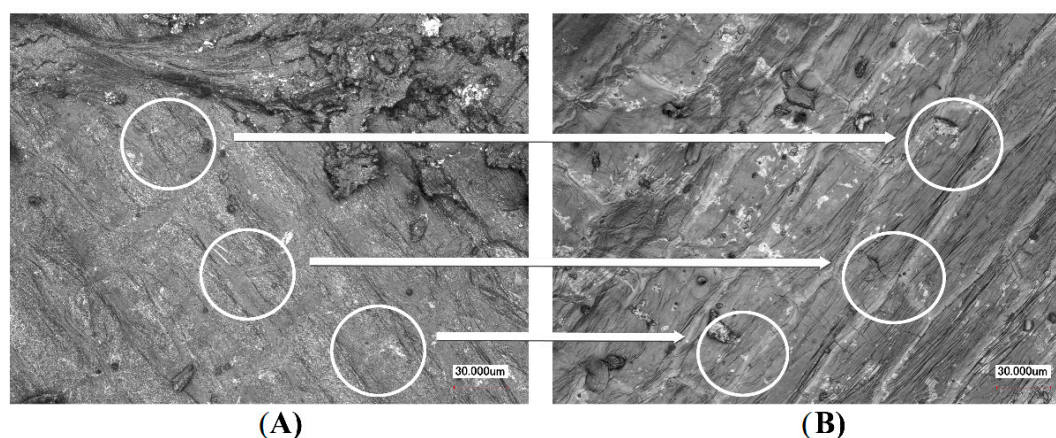
**Figure 2.** Morphology of surface: (**A**)—rice husk; (**B**)—biochar.

Determining the elemental composition showed the predominance of carbon in the rice husk biochar (Table 2). It was established that the degree of aromaticity of rice husk biochar was 0.36. There was also a high C:N ratio of 34.1. In addition, rice husk biochar had a high ash content: 12.7%.

The plots for Langmuir and Freundlich models obtained for Cu(II) adsorption on soil in pure form and soil with biochar are presented in Figure 3. Based on the coefficient of correlation values ($R^2$) obtained, it was observed that the Langmuir model best describes the adsorption of Cu(II) on the surface of studied samples (Table 3). The $C_m$ and $K_L$ values of soil for Cu(II) were 8.01 mM$\cdot$L$^{-1}$ and 29.76 L$\cdot$mM$^{-1}$, respectively. The addition of biochar obtained from rice husk led to an increase in the bond strength of metal with soil: the $K_L$ value increased 3.3 times. The values of $K_F$ in all cases were higher than the calculated values of $C_m$. In general, the use of both sorption models led to the same conclusion: the sequence of adsorbate location depending on the value of $C_m$, calculated according to the Langmuir equation, and $K_F$, according to the Freundlich equation, is similar (Table 3).
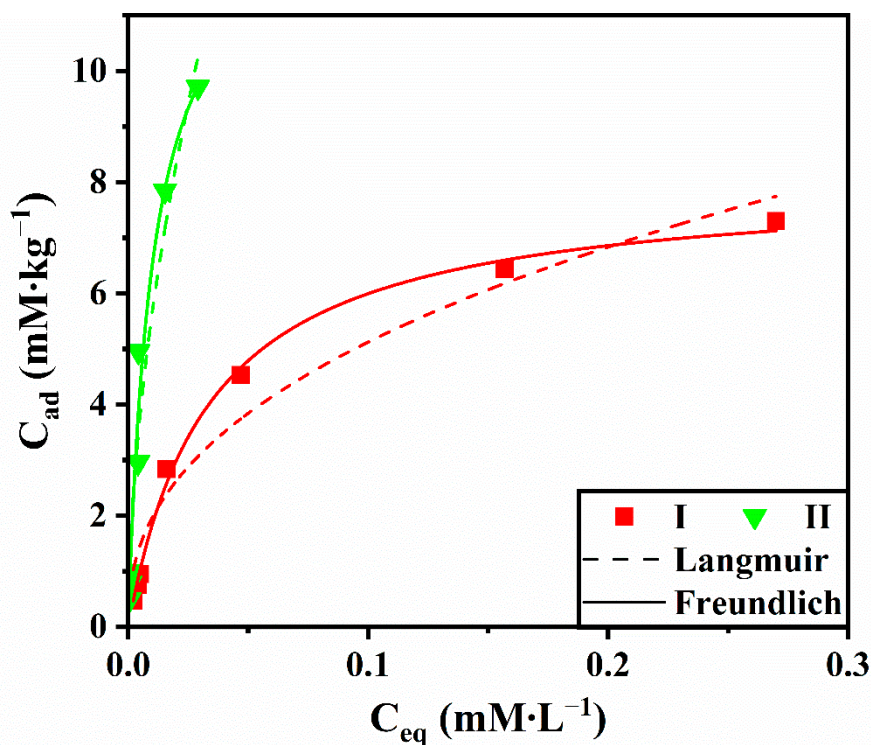
**Figure 3.** Adsorption isotherms of Cu(II) by soil in pure form (I) and soil with rice husk biochar (II).

**Table 3.** Fitted parameters for adsorption isotherms of Cu(II) by soil in pure form and with rice husk biochar.

| Sample | Langmuir | | | Freundlich | | |
|---|---|---|---|---|---|---|
| | $C_m$ (mM·L$^{-1}$) | $K_L$ (L·mM$^{-1}$) | $R^2$ | $K_F$ (L·kg$^{-1}$) | n | $R^2$ |
| Soil | 8.01 | 29.76 | 0.997 | 13.35 | 0.41 | 0.959 |
| Soil + biochar | 13.15 | 97.64 | 0.976 | 73.48 | 0.56 | 0.948 |

## 4. Discussion

Depending on the changing conditions of pyrolysis, the characteristics of the resulting biochar also changed. Various researchers have suggested that with an increase in the heating rate and final temperature of pyrolysis, the specific surface area of the biochar, its aromaticity, and its carbon content increase [24,27].

It was established that with increasing processing time at the first stage, a significant increase in the specific surface area was observed at the significance of product yield. A more complete saturation of biochar explains this effect with carbon. There was a more complete removal of volatile substances resulting from pyrolysis. Similar effects were also observed with an increase in the heating rate; however, they manifested themselves most strongly after an increase in the final pyrolysis temperature. This was due to the fact that many substances are thermally stable and removed at higher temperatures [24]. For example, a study by Kirti et al. [27] indicates that hemicellulose, cellulose, and lignin, the main components of lignocellulosic biomass, thermally decompose in their characteristic temperature ranges, which can be overlapped by other components. As a rule, thermal decomposition of hemicellulose occurs at a temperature of 190 to 380 °C, while cellulose decomposes at a temperature of 280 to 400 °C. Lignin (the most complex lignocellulosic component) varies thermally with temperature from 170 °C to over 800 °C. Based on the present study, it was found that the optimal conditions for obtaining biochar from rice husk included a heating rate of 11 °C·min$^{-1}$, a final temperature of 700 °C, and a holding time of 45 min (Table 1). Pyrolysis under the above conditions significantly transformed the structure of the rice husk. The network of small tubules in the rice husk was replaced

with a network of cells with high walls in the biochar (Figure 2). In addition, due to the deepening of the folds, the biochar surface became even more heterogeneous, and the number of potential sorption centers increased. However, the biochar retained a biogenic structure very similar to that of the original material.

The results of the study of the sorption characteristics of biochar obtained under optimal pyrolysis conditions indicated that this material has significant potential as a sorbent (Table 2). It should also be noted that the pore space of rice husk biochar was composed mainly of meso- and micropores. This feature makes biochar potentially effective when used in soils contaminated with heavy metals since it is micro- and mesopores that are primarily involved in the sorption of these pollutants [8].

According to elemental analysis data, biochar has a high degree of aromaticity, which indicates its potential stability in soil [24]. In addition, a high C:N ratio of 34.1 indicates that rice husk biochar will contribute to microbial nitrogen immobilization and, as a result, reduce greenhouse gas emissions and increase soil organic carbon [28]. The high ash content in this sorbent is due to the elemental composition of the raw material, which contains a large amount of silica.

The introduction of biochar obtained from rice husk into the soil led to an increase in the absorption capacity of the soil for Cu(II) (Figure 3, Table 3). The efficient sorption of metal in the biochar indicates that the studied sorbent sequestered the pollutant in itself. It has been shown that the mineral substances, alkaline metal ions, $\pi$-electrons, pore structures of micropores, abundant surface functional groups, and organic matters provide the binding sites for biochar remediation of HMs [29]. Biochar has the ability to sorb HMs in contaminated soil through precipitation, complexation, electrostatic attraction, and cation exchange of HMs from inorganic to organic states that vary the metals' motility and bioavailability [30]. Physical adsorption is mainly dependent on the surface properties such as specific surface area and pore structure. Electrostatic attraction between positively charged Cu(II) ions and the negatively charged biochar surface is the predominant mechanism of metal immobilization in the soils of the San Joaquin Valley [31]. Lei et al. confirmed that ion exchange is the main mechanism by which biochar from organic wastes fixes $Cu^{2+}$ [32]. Thus, the surface characteristics and special properties of biochar, such as large specific surface area and porosity, make it useful as an effective adsorbent in the remediation of soil polluted with HMs. The method of soil restoration with carbonaceous sorbents is currently gaining more and more popularity and shows high efficiency [16,33,34]. The conclusions drawn by different studies in terms of immobilization of HMs by biochar are inconsistent. The remediation effect of biochar is related to the types of HMs, soil types, and biochar application methods [35,36]. For example, biochar can effectively reduce water-soluble heavy metal contents in acid mining soil and the uptake of HMs in plants, but the effect of biochar is not notable for alkaline mining soil [37]. The effect of biochar produced from rice straw on Cd and Cu immobilization and bioavailability in soils with different acidity levels has been studied [38]. It was shown that rice straw biochar can be used for Cd pollution control in rice grain grown in paddy soil with varied acidity levels. However, further studies are needed on how biochar promotes Cu transport from rice root to shoot. Processing of agricultural waste to make biochar solves two problems: it makes efficient utilization of agricultural residues possible, and it allows for the creation of a valuable sorbent [39,40]. Problems that could arise from scaling may include logistical and warehouse difficulties, as well as the costs associated with pyrolysis of raw materials and embedding the resulting sorbent into the soil [41]. It is possible to reduce costs due to the low cost of raw materials.

## 5. Conclusions

Developing efficient, low-cost, and environmentally friendly technologies is crucial for sustainable biochar applications. A method for obtaining biochar from rice husk with desired characteristics was developed. The optimal pyrolysis parameters (heating rate, final heating temperature, and holding time) were established. The well-developed pore

structure of the obtained biochar allows it to be used as a potentially effective sorbent for the remediation of contaminated soils. It was also found that with a set holding time from 500 to 700 degrees, a heating rate from 8 to 11 °C·min⁻¹, and a holding time at a final temperature from 15 to 45 min, the specific surface area increased from 135 to 398 m²·g⁻¹, that is, practically 3 times. Pore distribution according to volume presented in the following order: mesopores > micropores > macropores in the obtained sorbent. The results of elemental analysis showed that carbon predominated in the sorbent (70.4%), and ring structures of carbon atoms were more prevalent than aliphatic structures. The degree of aromaticity suggests that the sorbent will be sufficiently stable when applied to soils for the purposes of soil restoration under chemical and long-term technogenic impact and may improve of the physical and biological properties of the soils. Adding the obtained biochar to the Haplic Chernozem increased the efficiency of Cu(II) adsorption. This study provides a theoretical, as well as practical, basis for the comprehensive evaluation of biochar in controlling HM contamination in soils. Further research should focus on developing robust mathematical models to optimize estimates of biochar sorption capacity and its application for different soil remediation scenarios. Predictive models are required to optimize soil restoration strategies and reduce biochar application costs by selecting the most suitable materials.

**Author Contributions:** Conceptualization, T.M., S.S., and S.M.; methodology, I.L., A.B., T.B., M.B., T.M., S.S., I.Z., and S.M.; formal analysis, I.L., A.B., A.T., and O.K.; investigation, I.L., A.T., and O.K.; resources, T.M., S.S., and S.M.; data curation, T.B., M.B., S.S., and S.M.; writing—original draft preparation, I.L. and V.D.R.; writing—review and editing, V.D.R., T.B., V.K., and M.B.; visualization, A.T. and I.L.; supervision, T.M.; project administration, T.B., M.B., and S.M.; funding acquisition, S.M., S.S., and T.M. All authors have read and agreed to the published version of the manuscript.

**Institutional Review Board Statement:** Not applicable.

**Informed Consent Statement:** Not applicable.

**Data Availability Statement:** Not applicable.

**Conflicts of Interest:** The authors declare no conflict of interest.

## References

1. Koptsik, G.N. Modern approaches to remediation of heavy metal polluted soils: A review. *Eurasian Soil Sci.* **2014**, *47*, 707–722. https://doi.org/10.1134/S1064229314070072.
2. Lu, Y.; Nakicenovic, N.; Visbeck, M.; Stevance, A.S. Policy: Five priorities for the UN sustainable development goals. *Nature* **2015**, *520*, 432–433. https://doi.org/10.1038/520432a.
3. Arunrat, N.; Sereenonchai, S.; Kongsurakan, P.; Hatano, R. Soil organic carbon and soil erodibility response to various land-use changes in northern Thailand. *Catena* **2022**, *219*, 106595. https://doi.org/10.1016/j.catena.2022.106595.
4. Lal, R.; Miller, F.P.; Logan, T.J. Are intensive agricultural practices environmentally and ethically sound? *J. Agric. Ethics* **1988**, *1*, 193–210. https://doi.org/10.1007/BF01833409.
5. Zwolak, A.; Sarzyńska, M.; Szpyrka, E.; Stawarczyk, K. Sources of Soil Pollution by Heavy Metals and Their Accumulation in Vegetables: A Review. *Water Air Soil Pollut.* **2019**, *230*, 164. https://doi.org/10.1007/s11270-019-4221-y.
6. Kumar, N.; Kumar, S.; Bauddh, K.; Dwivedi, N.; Shukla, P.; Singh, D.P.; Barman, S.C. Toxicity assessment and accumulation of metals in radish irrigated with battery manufacturing industry effluent. *Int. J. Veg. Sci.* **2015**, *00*, 1–13. https://doi.org/10.1080/19315260.2014.880771.
7. Nevedrov, N.; Protsenko, E. Technologies for optimization of ecosystem services and functions of soils under anthropogenic impact in urban areas. In *IOP Conference Series: Earth and Environmental Science*; IOP Publishing: Bristol, UK, 2018; Volume 177, p. 012009. https://doi.org/10.1088/1755-1315/177/1/012009.
8. Hu, R.; Xiao, J.; Wang, T.; Gong, Y.; Chen, G.; Chen, L.; Tian, X. Highly concentrated amino-modified biochars using a plasma: Evolution of surface composition and porosity for heavy metal capture. *Carbon* **2020**, *168*, 515–527. https://doi.org/10.1016/j.carbon.2020.07.012.

9.    Yanez Espinosa, L.; Briones Gallardo, R.; Flores, J.; Alvarez del Castillo, E. Effect of heavy metals on seed germination and seedling development of Nama aff. stenophylla collected on the slope of a mine tailing dump. *Int. J. Phytoremediation* **2020**, *22*, 1448–1461. https://doi.org/10.1080/15226514.2020.1781782.

10.    Tomei, M.C.; Daugulis, A.J. Ex situ bioremediation of contaminated soils: An overview of conventional and innovative technologies. *Crit. Rev. Environ. Sci. Technol.* **2013**, *43*, 2107–2139. https://doi.org/10.1080/10643389.2012.672056.

11.    Qin, G.; Gong, D.; Fan, M.Y. Bioremediation of petroleum-contaminated soil by biostimulation amended with biochar. *Int. Biodeterior. Biodegrad.* **2013**, *85*, 150–155. https://doi.org/10.1016/j.ibiod.2013.07.004.

12.    Huggins, T.M.; Haeger, A.; Biffinger, J.C.; Ren, Z.J. Granular biochar compared with activated carbon for wastewater treatment and resource recovery. *Water Res.* **2016**, *94*, 225–232. https://doi.org/10.1016/j.watres.2016.02.059.

13.    Liu, C.; Liu, F.; Ravnskov, S.; Rubæk, G.H.; Sun, Z.; Andersen, M.N. Impact of wood biochar and its interactions with mycorrhizal fungi, phosphorus fertilization and irrigation strategies on potato growth. *J. Agron. Crop Sci.* **2017**, *203*, 131–145. https://doi.org/10.1111/jac.12185.

14.    Suliman, W.; Harsh, J.B.; Abu-Lail, N.I.; Fortuna, A.-M.; Dallmeyer, I.; Garcia-Perez, M. The role of biochar porosity and surface functionality in augmenting hydrologic properties of a sandy soil. *Sci. Total Environ.* **2017**, *574*, 139–147. https://doi.org/10.1016/j.scitotenv.2016.09.025.

15.    Tang, J.; Zhu, W.; Kookana, R.; Katayama, A. Characteristics of biochar and its application in remediation of contaminated soil. *J. Biosci. Bioeng.* **2013**, *116*, 653–659. https://doi.org/10.1016/j.jbiosc.2013.05.035.

16.    Guo, M.; Song, W.; Tian, J. Biochar-facilitated soil remediation: Mechanisms and efficacy variations. *Front. Environ. Sci.* **2020**, *8*, 521512. https://doi.org/10.3389/fenvs.2020.521512.

17.    Sushkova, S.; Minkina, T.; Dudnikova, T.; Barbashev, A.; Mazarji, M.; Chernikova, N.; Lobzenko, I.; Deryabkina, I.; Kizilkaya, R. Influence of carbon-containing and mineral sorbents on the toxicity of soil contaminated with benzo [a] pyrene during phytotesting. *Environ. Geochem. Health* **2022**, *44*, 179–193. https://doi.org/10.1007/s10653-021-00899-x.

18.    Karam, D.S.; Nagabovanalli, P.; Rajoo, K.S.; Ishak, C.F.; Abdu, A.; Rosli, Z.; Muharam, F.M.; Zulperi, D. An overview on the preparation of rice husk biochar, factors affecting its properties, and its agriculture application. *J. Saudi Soc. Agric. Sci.* **2022**, *21*, 149–159. https://doi.org/10.1016/j.jssas.2021.07.005.

19.    Li, Y.; Ding, X.; Guo, Y.; Rong, C.; Wang, L.; Qu, Y.; Ma, X.; Wang, Z. A new method of comprehensive utilization of rice husk. *J. Hazard. Mater.* **2011**, *186*, 2151–2156. https://doi.org/10.1016/j.jhazmat.2011.01.013.

20.    Li, A.; Xie, H.; Qiu, Y.; Liu, L.; Lu, T.; Wang, W.; Qiu, G. Resource utilization of rice husk biomass: Preparation of MgO flake-modified biochar for simultaneous removal of heavy metals from aqueous solution and polluted soil. *Environ. Pollut.* **2022**, *310*, 119869. https://doi.org/10.1016/j.envpol.2022.119869.

21.    Farhana, A.; Alias, A.; Talib, N.; Rashid, Z.; Ghani, W.A.W.A.K. Characteristics of rice husk biochar blended with coal fly ash for potential sorption material. *Malays. J. Anal. Sci.* **2018**, *22*, 326–332. https://doi.org/10.17576/mjas-2018-2202-19.

22.    Tag, A.T.; Duman, G.; Ucar, S.; Yanik, J. Effects of feedstock type and pyrolysis temperature on potential applications of biochar. *J. Anal. Appl. Pyrolysis* **2016**, *120*, 200–206. https://doi.org/10.1016/j.jaap.2016.05.006.

23.    Li, S.; Harris, S.; Anandhi, A.; Chen, G. Predicting biochar properties and functions based on feedstock and pyrolysis temperature: A review and data syntheses. *J. Clean. Prod.* **2019**, *215*, 890–902. https://doi.org/10.1016/j.jclepro.2019.01.106.

24.    Burachevskaya, M.; Minkina, T.; Zamulina, I.; Fedorenko, A.; Kalinichenko, V.; Lobzenko, I.; Sushkova, S. Effect of biochar on the lead mobility in Haplic Chernozem. In *IOP Conference Series: Earth and Environmental Science*; IOP Publishing: Bristol, UK, 2020; Volume 578, p. 012012. https://doi.org/10.1088/1755-1315/578/1/012012.

25.    McClements, D.J. The future of food colloids: Next-generation nanoparticle delivery systems. *Curr. Opin. Colloid Interface Sci.* **2017**, *28*, 7–14. https://doi.org/10.1016/j.cocis.2016.12.002.

26.    Ayawei, N.; Ebelegi, A.N.; Wankasi, D. Modelling and interpretation of adsorption isotherms. *J. Chem.* **2017**, *2017*, 3039817. https://doi.org/10.1155/2017/3039817.

27.    Yuan, H.; Lu, T.; Wang, Y.; Huang, H.; Chen, Y. Influence of pyrolysis temperature and holding time on properties of biochar derived from medicinal herb (radix isatidis) residue and its effect on soil CO2 emission. *J. Anal. Appl. Pyrolysis* **2014**, *110*, 277–284. https://doi.org/10.1016/j.jaap.2014.09.016.

28.    Kirti, N.; Tekade, S.P.; Tagade, A.; Sawarkar, A.N. Pyrolysis of pigeon pea (Cajanus cajan) stalk: Kinetics and thermodynamic analysis of degradation stages via isoconversional and master plot methods. *Bioresour. Technol.* **2022**, *347*, 126440.

29.    Ji, M.; Wang, X.; Usman, M.; Liu, F.; Dan, Y.; Zhou, L.; Campanaro, S.; Luo, G.; Sang, W. Effects of different feedstocks-based biochar on soil remediation: A review. *Environ. Pollut.* **2022**, *294*, 118655. https://doi.org/10.1016/j.envpol.2021.118655.

30.    Wang, M.; Zhu, Y.; Cheng, L.; Andserson, B.; Zhao, X.; Wang, D.; Ding, A. Review on utilization of biochar for metal-contaminated soil and sediment remediation. *J. Environ. Sci.* **2018**, *63*, 156–173. https://doi.org/10.1016/j.jes.2017.08.004.

31.    Uchimiya, M.; Chang, S.; Klasson, K.T. Screening biochars for heavy metal retention in soil: Role of oxygen functional groups. *J. Hazard. Mater.* **2011**, *190*, 432–441. https://doi.org/10.1016/j.jhazmat.2011.03.063.

32.    Lei, S.; Shi, Y.; Qiu, Y.; Che, L.; Xue, C. Performance and mechanisms of emerging animal-derived biochars for immobilization of heavy metals. *Sci. Total Environ.* **2019**, *646*, 1281–1289. https://doi.org/10.1016/j.scitotenv.2018.07.374.

33.    Wang, Y.; Wang, H.S.; Tang, C.S.; Gu, K.; Shi, B. Remediation of heavy-metal-contaminated soils by biochar: A review. *Environ. Geotech.* **2019**, *9*, 135–148. https://doi.org/10.1680/jenge.18.00091.

34. O'Connor, D.; Peng, T.; Zhang, J.; Tsang, D.C.; Alessi, D.S.; Shen, Z.; Bolan, N.S.; Hou, D. Biochar application for the remediation of heavy metal polluted land: A review of in situ field trials. *Sci. Total Environ.* **2018**, *619*, 815–826. https://doi.org/10.1016/j.scitotenv.2017.11.132.

35. El-Naggar, A.; Shaheen, S.M.; Ok, Y.S.; Rinklebe, J. Biochar affects the dissolved and colloidal concentrations of Cd, Cu, Ni, and Zn and their phytoavailability and potential mobility in a mining soil under dynamic redox-conditions. *Sci. Total Environ.* **2018**, *624*, 1059–1071. https://doi.org/10.1016/j.scitotenv.2017.12.190.

36. Gu, J.; Yao, J.; Duran, R.; Sunahara, G.; Zhou, X. Alteration of mixture toxicity in nonferrous metal mine tailings treated by biochar. *J. Environ. Manag.* **2020**, *265*, 110511. https://doi.org/10.1016/j.jenvman.2020.110511.

37. Alvarez-Rogel, J.; Gomez, M.D.T.; Conesa, H.M.; Parraga-Aguado, I.; Gonzalez-Alcaraz, M.N. Biochar from sewage sludge and pruning trees reduced porewater Cd, Pb and Zn concentrations in acidic, but not basic, mine soils under hydric conditions. *J. Environ. Manag.* **2018**, *223*, 554–565. https://doi.org/10.1016/j.jenvman.2018.06.055.

38. Chen, L.; Guo, L.; Liao, P.; Xiong, Q.; Deng, X.; Gao, H.; Zhang, H. Effects of biochar on the dynamic immobilization of Cd and Cu and rice accumulation in soils with different acidity levels. *J. Clean. Prod.* **2022**, *372*, 133730. https://doi.org/10.1016/j.jclepro.2022.133730.

39. Tsai, W.T.; Chang, C.Y.; Wang, S.Y.; Chang, C.F.; Chien, S.F.; Sun, H.F. Utilization of agricultural waste corn cob for the preparation of carbon adsorbent. *J. Environ. Sci. Health Part B* **2001**, *36*, 677–686. https://doi.org/10.1081/PFC-100106194.

40. Shehrawat, P.S.; Sindhu, N. Agricultural waste utilization for healthy environment and sustainable lifestyle. *Ann. Agric. Biol. Res.* **2015**, *20*, 110–114.

41. Kalus, K.; Koziel, J.A.; Opaliński, S. A review of biochar properties and their utilization in crop agriculture and livestock production. *Appl. Sci.* **2019**, *9*, 3494. https://doi.org/10.3390/app9173494.